Proceedings, 17th. U.S.-Japan Bridge Engineering Workshop, Nov. 12-14, 2001, Public Works Research Institute, Japan, Technical Memorandum of PWRI No. 3843, Hiroshi Sato, Ed. pp. 579-594, PWRI, 2002.

CORROSION OF POST-TENSIONED TENDONS IN FLORIDA BRIDGES

Rodney G. Powers[1] Alberto A. Sagüés[2] and Yash Paul Virmani[3]

Abstract

Severe corrosion distress and failures in post-tensioned tendons has been found in two major bridges in the State of Florida. Corrosion distress and complete tendon failure has been identified in horizontally oriented tendons that support pre-cast bridge superstructure box segments. In virtually all instances, the observed corrosion has been associated with the presence of grout voids and visual evidence of grout bleed water having been present for indeterminate periods of time. With few exceptions, corrosion induced strand failures have occurred in the immediate vicinity of the anchorage. The anchorage systems in both bridges utilize a proprietary multi-plane anchorage (housing) comprised of ductile cast iron and forged steel wedge plate. The presence of these metals coupled with high strength strands gives rise to concerns relative to galvanic corrosion thus prompting this preliminary investigation focusing on dissimilar metals corrosion. The investigation involves laboratory tests that examine the corrosion aspects of grout bleed water and re-charge water in contact with dissimilar metals comprising the tendon and anchorage system. The preliminary results indicate that the high strength post-tensioned strands are mostly anodic to the anchorage system when exposed to either grout bleed water or recharge water such as that which may be experienced through leakage. The preliminary findings of the investigation are presented along with the implications on existing structures and on future design and materials selection for post-tensioning systems.

Introduction

Commencing in 1979 with the construction of five major bridges in the Florida Keys, the Florida Department of Transportation (FDOT) now has an inventory of more than 80 major bridges that utilize this type of construction. Both bonded (internal) and non-bonded (external) tendons have been utilized for both substructure and superstructure components on inland as well as coastal marine structures. Typically, these are large structures (>750 meters in length) that span either large bodies of coastal waters or large
highway interchanges. Each of Florida's structures was designed and built using what was considered state-of-the-art materials and construction practices for the time.
The potential for corrosion of tendons in bridges in the United States has been recognized. In 1989, a study was commissioned by the United States Department of Transportation, Federal Highway Administration to examine the performance of grouts

---

[1]Assistant State Corrosion Engineer, Florida Dept. of Transportation, Gainesville
[2]Distinguised Professor, Dept. of Civil and Environmental Engineering, University of South Florida, Tampa
[3]Research Chemist, U.S. Department of Transportation, Federal Highway Administration, McLean, Virginia

for post-tensioned bridge structures. In the final report (Ghorbanpoor, 1993) it was demonstrated that conventionally used grout materials were susceptible to development of significant levels of bleed-water under normal handling conditions. It was shown that grout bleed-water tended to rise and collect in the upper reaches of test specimens comprised of a single strand in a vertically positioned grouted duct. Further, it was shown that although the bleed-water eventually dissipated, significant corrosion developed on the strand at the grout-water interface. It was further shown that one particular, commonly used grout containing an aluminum based grout-expanding admixture experienced the highest amounts of bleed-water development and subsequent corrosion. Similarly, severe corrosion distress has been observed in cyclically loaded full-scale tendon mock-up specimens (Tabatabai, et al., 1995) within only one to two months' exposure to grout bleed-water.

Corrosion of post-tensioned strands has been identified in two Florida Bridges. The first reported incident was at the Niles Channel Bridge (NC) in the Florida Keys (Powers 1999) followed by Mid Bay Bridge (MBB) in the Western panhandle (Corven, 2000). The superstructure of both bridges utilizes non-bonded (external) tendons arranged in a configuration such that the center lengths of the tendons are draped downward from the anchorages through deviation blocks along the length of the spans (Figure 1). The anchorage assembly is depicted in Figure 2. In both structures, the tendons failed in the anchorage region (Figure 3).

Of particular interest in this laboratory investigation was the common factors amongst the two bridges that have experienced corrosion upon the tendons. These common factors include, (i) corrosion was mainly at or near the anchorages; (ii) the anchorages utilize ductile cast iron anchors and forged steel wedge plates; (iii) corrosion was always associated with grout voids (Figure 4), the presence of grout bleed-water and soft, chalky grout in the affected areas; and (iv) corrosion was always (except for one instance) associated with grout that contained only trace (background) levels of chloride. These common factors give rise to the possibility of galvanic action (dissimilar metal corrosion) taking place between the post-tensioning strand and the milder steel anchorage components in the presence of grout bleed-water or infiltrating (recharge) water. The preliminary experiments in this work explore the corrosion behavior of the metal the metal components comprising the anchorage system when exposed to grout bleed-water and re-charge water.

Experimental Details:

Grout: Grout mixes were made to replicate the aluminum admixed grout used at MBB. The grout consisted of Type I Portland cement with 1 percent (by weight) aluminum based expanding admixture and a water to cement ratio of 0.45. A control mix of the same proportions was made that did not contain the aluminum based expanding admixture. These grouts were subjected to standard tests (ASTM C940-98a) to establish percentages of bleed-water development and shrinkage. Additionally, these grouts were separately subjected to the same standard test but with the introduction of vibration during the plastic phase of the grout. The vibration was introduced by placing the test specimens directly upon a laboratory concrete vibrating table. The peak amplitude of the vibration was <0.10mm at 60Hz. This aspect was introduced in an attempt to generate the same magnitude of grout bleed water development in the laboratory specimens as that which had been observed in the field.

Anchorage Mock-up Details: The mock-up utilized a proprietary anchorage system (Figure 2) of the same type and from the same manufacturer as that used at MBB. The system consists of a ductile iron, multi-plane anchor manufactured to ASTM A27, Grade 65-45-12 specifications and a forged steel wedge plate manufactured to ASTM A688 specifications. The post-tensioning strands were seven-wire, 14.3mm nominal strand diameter, Grade 1860 manufactured to AASHTO M 203 specifications. Composition of the components was verified via metallographic examination and spectrographic analysis. The wedge plate in this experiment was represented by a cut-off piece of plate cast into the anchorage grout. The wedge plate section measured 5.5cm wide (the thickness of the plate) by 12.7cm in length. Since this specimen was cut from the edge of the wedge plate, one side of the test specimen had a sawn edge while one side was in the "as-manufactured condition". The total surface area of the portion of the specimen in contact with grout was approximately 81cm^2. This metal-to-grout surface contact area is proportionate to the contact area that would exist with a horizontally positioned anchor approximately 50% filled with grout. The surface area of the anchor in contact with the grout was 856cm^2. All of the metal components used in the experiment were "as-new" and showed no signs of deterioration or contamination. The strands were gray in color, free of grease and oils and had a mill finish.

The mock-up (Figures 5 and 6) consisted of seven bundled, seven-wire strands and a cut-off section of the wedge plate cast into the anchorage in a vertical position. A thick grout made up of cement and micro-silica was used to seal the bottom 4cm of the anchorage. Care was used to ensure that none of the metal components were in contact with one another. The grout used in this experiment was as previously described using 1 percent (by weight) aluminum based expanding admixture. Approximately 3.3L of grout was placed into the anchor. The grout filled the anchor to a point 3cm from the top (outer end). During grout placement, the strands and wedge plate section were suspended in place using cloth tie-wires. Following introduction of the grout, the specimen was vibrated (as indicated earlier) continuously for four hours. Subsequently, measurements were made for grout shrinkage and bleed-water. Each of the metallic components was equipped with securely attached and sealed electrical connections to facilitate testing and establishing electrical continuity between the anchorage components. Two activated titanium rods (3.2mm diameter) were imbedded into the grout. One rod was 10cm in length; the other was 4cm in length. These served as counter and reference electrodes in the polarization resistance tests. The open end of the anchor was fitted with a suitably sized glass vessel to minimize evaporation during the laboratory evaluation. A silicone seal approximately 2mm thick by 25mm wide was used between the glass vessel and anchor. A section measuring 10mm wide was cut out of the silicone seal to replicate a defect in construction that would be of sufficient size to allow water re-charge and aeration similar to that which might be experienced in actual field conditions.

Corrosion Testing of the Anchorage Mock-up: Tests consisted of (i) half-cell potential measurements, (ii) macrocell current measurements, and (iii) polarization resistance measurements.

Half-cell potential measurements were taken of the individual metal components and of the coupled components using a copper-copper sulfate reference electrode (CSE) and high

impedance voltmeter. These measurements were taken by first removing the glass vessel and then placing the reference electrode directly in contact with the grout. Except as otherwise noted, all half-cell potential measurements of individual components (anchor, wedge-plate section and strands) were taken instantaneously (within one second) after interruption of the electrical connection to other components. The anchor and wedge plate (referred to as "anchorage" or "anchorage components") remained electrically coupled throughout the experiment. Macro-cell current between the individual components was measured using a low resistance digital ammeter.

As shown in Table 1, five water re-charge events were completed. Water re-charging consisted of adding 100-200ml de-ionized water to the top of the specimen. Typically, following each re-charge event, measurements of potentials and current were made until all of the metal components either reached a passive condition, or the macro-cell current reached near steady-state values (as in the fourth recharge event). At day 105, polarization and electrochemical impedance spectroscopy (EIS) tests were made on the individual components and with all components electrically coupled. Polarization resistance tests were conducted for the fourth and fifth recharge events. In the fifth re-charge event, the distilled water contained 1,000ppm chlorides. The purpose of the chloride addition was to simulate re-charge water such as that which might occur from bridge deck run-off water in a marine environment. This chloride value was selected based on actual field tests on rainwater run-off from a bridge over Tampa Bay (Florida). Grout chloride content determinations were made using standard potentiometric methods.

Post-testing Examination: After completion of the corrosion tests, the specimen was dismantled and subjected to visual examination. The specimen was dismantled by first saw-cutting lengthwise through the anchor, two cuts situated 180 degrees from one another. This allowed the anchor to be easily removed without disturbing its contents. The grout in the mock-up was first scored (using an abrasive wheel saw) and then easily separated from the components that had been cast into it. The pH of the grout was measured at various locations throughout the specimen using liquid, color reactive reagents. Three of the seven-wire strands were randomly selected for detailed examination. The remaining four strands were preserved for possible subsequent evaluation. The selected strands were first cleaned by wire brushing while rinsing in distilled water followed by forced air-drying to minimize further rust development. The individual wires were numbered along with markings to later identify wire orientation (position) in the strand. This allowed for identification of the position of corrosion on individual wires after the strand wires were separated. After the markings were applied, the individual wires were separated from each of the three selected strands. The visual condition of each wire was determined followed by furthe cleaning using the methods previously described. Measurements of pit depth on the individual strand wires were made using precision digital micrometers (needle point for pits, square jaws for non-corroded areas). These measurements were made by first measuring the full cross-sectional diameter of the individual wire in the immediate, non-corroded area nearest the location of the metal loss (within 1cm). Care was used to take both measurements across the same cross-sectional plane to minimize the effects of any out-of-round conditions that may exist. Maximum measured pit depths were plotted on cross sectional drawings showing position and measured corrosion loss. The condition of the anchor interior and wedge plate section was visually characterized after first cleaning the components as previously described. The components were then examined under 6X magnification at which time metal

surface attack was semi-quantitatively determined by direct measurements of pits and surface wastage.

Results and Observations:

Standard Grout Tests: In these standard tests (Figure 7) grout shrinkage is characterized by the loss of grout volume due to water loss (grout bleed-water) during the plastic phase. Results of these tests showed grout shrinkage and bleed-water volumes to be within expected parameters for the aluminum admixed specimen, and the non-admixed control specimen. However, when these materials were exposed to low amplitude vibration as previously described, the volume of bleed water increased dramatically. The non-vibrated control specimen developed 1.81% bleed-water, and the vibrated specimen developed 6.2% bleed-water. Comparatively, the aluminum admixed specimens developed 1.94% bleed-water (non-vibrated) and 10.2% bleed-water (vibrated) with a correspondingly equal loss of grout volume. Visual examination of the test specimens (except for the vibrated, aluminum-admixed specimen) showed the grout to be of relatively uniform consolidation and coloration throughout. Comparatively, the aluminum admixed specimen showed wide variations in coloration (Figure 8) along its length. The lower portion of the specimen was dark and dense in appearance but with increasing height, the grout was increasingly lighter in coloration until finally at the uppermost portion of the specimen (~1cm) the grout was near white in color and chalky in texture (Figure 9). The pH of the grout at the top of the specimen was determined to be 8.7 (+/- 0.5). The pH of the grout near the bottom of the specimen was >~12.

Grout in the Experimental Anchorage Mock-up: The bleed-water that developed as a result of intentional vibration reached a depth of about 1.25cm (7.6% by volume) with a correspondingly equal grout volume loss. The pH of the bleed-water was >12.2. After 24 hours of curing, the grout at the top of the specimen consisted of a wet, pasty, chalk-like layer that typically varied in thickness from 2 to 5mm. At this time, only trace amounts of free bleed water remained on the top of the specimen. The pH of the chalky grout top surface was measured at 8.7 (+/- 0.5). Analysis of the same chalky material (measured prior to adding re-charge water) showed the chloride content to be 440ppm while post-experimental analysis of the grout near the bottom of the specimen was 69ppm. This lower value is consistent with expected baseline values.

Corrosion Behavior in the Experimental Anchorage Mock-up: Portions of the coupled metallic components in the freshly cast system were initially in the active condition, as shown one day after casting by a combined potential of –302 mV and macrocell current of –70 μA (negative sign assigned to indicate the strand was anodic). Five days later the potentials had become 60 mV more positive and the macrocell current decayed to –9μA, indicating a combination of increased passivity and drying. On day six, the first of five water re-charge events commenced and evaluation was carried out over a period of nearly six months.

Table 1 summarizes the main results, to which the following notes apply. *Event No. 1:* After measurements during this event were completed, the glass vessel was placed on top of thus

reducing the rate of evaporation; *Event No. 2:* In this and in the following events, there was a brief period after water recharge where the strands were cathodic to the rest of the assembly. However, most of the integrated macrocell charge was transferred while the strands were the anodic part of the macrocell. *Event No. 3:* Beginning on day 83, about one month since starting this event, the strands were electrically detached from the anchor and wedge plate section. The anchor and wedge plate were left electrically coupled and the glass vessel was removed from the specimen. The purpose of these steps was to simulate drier conditions. Electrochemical tests conducted at day 106 indicated greatly reduced corrosion intensity. The specimen was left with the components in an electrically discontinuous condition and with the glass vessel removed until day 113 when the next event started; *Event No. 4:* The glass top was replaced after the components were interconnected again on day 114. *Event No. 5:* Figure 10 shows the macrocell current development during this event. The specimen remained with all components coupled and the glass top in place until day 166 when the experiment ended.

Dismantling and Examination of the Anchorage Mock-up Components:

Condition of the Anchor: The grout in the mock-up showed no indication of adhesion to the interior surface of the anchor. The interior surface of the anchor was found to be completely unaffected during the experiment except for corrosion that developed around its circumference beginning at approximately 0.5cm below the top grout level and extending upward approximately 2cm. The region above the grout level experiencing corrosion was that area that was wetted via direct contact with re-charge water and capillary rise during the experiment. This area had widespread surface corrosion attack that typically penetrated the surface approximately 0.25mm. The surface area in this zone affected by generalized corrosion was estimated at 80%. Infrequent pitting attack was also present. The pits were approximately 1mm wide and variable in depth up to 1.5mm.

Condition of the Wedge-plate Section: The surface of the metal in contact with the grout was found to be unaffected during the experiment except for an area beginning approximately 1cm below the top grout level and extending upward approximately 2cm. Under 6X magnification, the affected zone on the "as manufactured" surface showed localized pitting in the form of elongated grooves approximately 2mm wide and 1mm to 2mm deep; one area was 5mm in length and the other was 12mm in length. (The lengthwise direction followed the grout line.) The affected area of the saw-cut surface showed light surface wastage accompanied by the presence of nine mostly circular pits 1mm to 3mm wide and 0.5 to 1mm deep. The location of these pits was generally equally distributed above and below the area coinciding with the top of the grout.

Condition of the Strands: The surfaces of the strands in contact with the grout were found to be unaffected during the experiment except for the area beginning approximately 2.5cm below the top of the grout and 2cm above the top of the grout. The area beginning approximately 2cm above the top of the grout and extending downward to approximately 1cm below the grout had heavy deposits of red to dark brown colored corrosion products (Figure 11). Extensive corrosion pitting was noted on the wire surfaces in the area coinciding with ~0.5cm above and below the top of the grout. The grout immediately adjacent to the strands in the zone beginning at the top of the grout and extending downward approximately 3cm was soft and chalky and the pH was

measured at 8.7 (+/-0.5). The individual wires of the three selected strands were separated for further examination. The previously mentioned corrosion pitting (near the top of the grout) was confined entirely to the outer surfaces of the individual wires. Although multiple pits existed along this ~1cm long affected zone, the area of heaviest attack was mostly centered at the area coinciding with the top of the grout. The typical appearance of the pitted areas is depicted in Figure12, and a schematic representation of the maximum measured pit depth and relative sizes of the pits is presented (Figure 13) for each of the three strands examined.

Discussion

The field corrosion incidents showed that while large portions of the strands and anchorage components remained in the passive state, intense localized corrosion did take place leading to enough loss of tendon cross section to result in mechanical failure. The passive behavior of most of the steel is as expected from the highly alkaline nature of the grout pore water. The presence of localized corrosion indicates either severe chloride contamination, or a marked local reduction in the pH of the water in contact with the steel, or a combination of both (Li 2001). Once initiated, localized corrosion could be seriously aggravated by electrochemical coupling of the small anodic area with a large cathodic region (Kranc 2001).

The corrosion was present near anchorages and by bleed water voids, which led to speculation on how the requisites for localized corrosion indicated above may have developed. It was thought that a lowered pH could develop at the interface between the grout and the void area by reaction with CO_2 leaking in from the external atmosphere. Furthermore, chloride concentration increases may occur there by penetration into the void area by salty runoff from the bridge surface, or by evaporative concentration of the bleed water (which should contain chlorides leached from the background amount allowed by the grout specifications) initially in the void. Aggravation of the corrosion could result if the anchorage or wedge plate were particularly efficient cathodes. The preliminary experiments in this work aimed to establish the likelihood of those speculative mechanisms.

The standard grout test results confirmed the tendency of grouts such as those used in the affected bridges to develop large bleed water regions near the anchorages, especially in the presence of modest vibration amplitudes that may exist during normal construction operations. The transition zone between grout and simulated void space in the experimental anchorage mock up was exposed to ambient air through the silicone seal cut out, which allowed for some evaporation and external air access. As anticipated, a lowered pH (~9) in that zone was observed consistent with carbonation of the hydrated cement present there by exposure to atmospheric CO_2, which could happen in a short time considering the highly porous nature of that chalky material (Moreno 1998). Furthermore, the chloride content there (before any intentional salt contamination) was ~ 6 times greater than in the bulk of the grout indicating that a chloride concentration mechanism, possibly evaporative concentration as speculated, was active.

Post-experiment analysis indicated that most of the corrosion developed at or around the grout/simulated void interface, while the rest of the assembly in contact with grout showed the typical appearance of passive steel in concrete. The latter behavior was as expected, since the total chloride contamination (even after addition of 200ml of 1000 ppm Cl^- water in the last

recharge event) was not enough to initiate widespread corrosion considering the relatively large volume of highly alkaline grout involved (Li 2001). Likewise, corrosion at the interface was not surprising as conditions there were much more propitious to corrosion initiation. In that zone, the lower pH and higher chloride content substantially elevated the $[Cl^-]/[OH^-]$ ratio compared to the bulk of the grout (Li 2001). The electrochemical measurements provided confirming evidence of the presence of active steel/iron behavior by observation of highly negative potentials (Bentur 1997) and correspondingly high corrosion current from Rp tests as well as high macrocell currents. These indications were more pronounced early during each recharge event when water was plentiful at the transition zone. As water absorption and evaporation ensued the mixed potential evolved toward values indicative of a less predominant active region. Near the end of the test period (Recharge Events No. 4 and 5), corrosion was maintained over long time periods with minimal water addition, sustained by retained moisture in the anchorage. The corrosion proceeded at a substantial rate (see below) even though total external chloride contamination was modest.

Corrosion of the strands (penetration depth as much as ~7% of a wire diameter) was severe in view of the relatively short duration of the tests and the low tolerance of a loaded system to localized reductions in cross section (Stauder 1998, Vermaas 2001). The corrosion morphology of the strands (Figure 12) is consistent with that of shallow pitting, constrained to a small region by local acidification from hydrolysis of ejected metal cations (Jones 1996), and protection of the surrounding region by local potential depression (Pedeferri 1996). An order-of-magnitude estimate of the total amount of corrosion in the strands can be made by assuming that each outer strand wire had an equivalent integrated pitted area ~10 mm^2 with a depth ~0.23 mm (average depth from Figure 13). For 6 corroding wires in the 7 strands this corresponds to a total metal loss of ~100 mm^3, or an anodic charge of ~2,600 C if the steel corroded as Fe^{++}. This value may be contrasted with the integrated value over time of the anodic macrocell current data in Figure 10 (the longest recharge event), which yields ~1,200 C. While the corrosion charge estimate is subject to considerable uncertainty, the similarity of the macrocell and corrosion charges suggests that galvanic coupling with the anchorage accounted for much of the metal loss at the strands. Nominal corrosion current estimates from polarization resistance tests (Table 1) are available for moist conditions only for instances when the strands were cathodic early in recharge events 4 and 5. Nevertheless, these results also illustrate cases where the macrocell currents (304 μA and 136 μA) were a significant fraction of the estimated local cell action at the strands (749 μA and 875 μA respectively).

Both the anchor and the wedge plate had actively corroding spots, experiencing a total amount of corrosion comparable or greater than that experienced by the strands. However, the measurements of the "off" potential and the direction of the macrocell current showed that the combined anchor and wedge plate section developed a mixed potential sufficient to act as an efficient net cathode except for the short periods when there was free recharge water over the grout. The available data do not permit identifying which of those two components was the most cathodic but the ductile iron anchor with its large surface area, as-cast finish and high carbon and silicon content deserves consideration for that role.

The findings from the field and the laboratory experiments discussed above showed that severe localized corrosion can develop in post-tensioned tendons at voids left by receding bleed water, even with very mild external chloride contamination. Pitting penetration on the order of that observed here after only ½ year of exposure to the laboratory conditions (up to 0.35 mm) already has some significant adverse effects, as it has been reported to reduce by half the ductility of tensioned bridge wires (Vermaas, 2001). A rough indication of the time required for outright overload failure can be made by conservatively assuming that the terminal stress in post tensioned strands for the application of interest is on the order of 70% of the ultimate tensile strength. Failure is likely to occur before corrosion reduces the local cross section by 30%, since the pit shape introduces severe stress concentration not necessarily compensated by notch strengthening (besides possible embrittlement effects from any hydrogen generation at the corroding region) (Stauder1998, Vermaas 2001). An ~20% reduction in cross section (which may result from a broad pit ~1.5 mm deep) could easily be above the tolerable limit. If pit depth were to increase linearly with time at a rate of 0.35 mm per ½ year (for the deepest pit in Figure 12), the first wire failures could then develop after ~2 years of exposure to conditions such as those simulated in the laboratory. Longer times would be required if the pit penetration is proportional to a lower power of time (e.g. ~4 years or ~8 years for ½ or 1/3 power dependence as is common in other systems (Szklarska-Smialowska 1986). While these estimates are subject to much uncertainty and dependent on conditions such as the occurrence of periodic recharge events, the results are in the order of the ages of the bridges considered here at the time they were affected by tendon failures.

The findings indicated above are preliminary in nature but serve to formulate a working picture of the events leading to the failures observed in the field, and as a guide to implement initial corrosion prevention measures. It is clear that bleed water voids can be a major source of corrosion tendon failure, and that failure can develop over a very short time frame. Rigorous implementation of bleed water avoidance measures is essential in new construction, as well as avoiding design that may promote galvanic corrosion of the strands. Thorough examination of existing structures to detect and remedy voids is in order. Remediation of voided anchorages or tendons that do not show significant corrosion must be made in a manner that will not introduce or reactivate further corrosion. Aspects revealed but only partially addressed in this work (e.g., the cathodic efficiency of anchorages versus wedge plate, the extent and mechanism of pH reduction at the grout/void interface, and the factors determining the anodic nature of the strand with respect to the other metallic components) are presently being examined in detail in an ongoing investigation and will be reported in the future.

Conclusions

1. Severe corrosion of steel strands was encountered in post-tensioned tendons of two major bridges in the State of Florida. The corrosion was associated with grout bleed-water voids and chloride ion contamination, in regions of the superstructure where periodic water intrusion was likely.

2. Grout tests indicated that modest vibration (as it may be encountered under normal construction conditions) could dramatically increase the amount of bleed water developed by the types of materials used in the bridges affected by corrosion.

3. Severe corrosion developed over six months testing in a laboratory anchorage mock-up where standard high strength steel strands and ductile iron and carbon steel anchorage components were partially in contact with hardened grout, and subject to periodic water recharge with and without moderate chloride ion contamination.

4. Electrochemical measurements indicated that portions of the strand and of the anchorage component surfaces became active upon water recharge and stayed active for extended periods afterwards, even without addition of chloride ions. Direct observation showed that corrosion took place in the transition zone between grout and air space, while the metal completely embedded in grout remained in the passive condition.

5. The grout in the transition zone had reduced pH and increased chloride content compared with the grout in the bulk. This situation appears to be the result of evaporative concentration of the initial bleed water and superficial carbonation upon contact with CO_2 in the air. These conditions promoted depassivation and subsequent corrosion damage of the metallic components at the grout transition zone.

6. Corrosion at the transition zone was aggravated by galvanic coupling between the small active area and the large passive metal area on contact with the bulk of the grout. Electrochemical measurements indicated that for most of the time the anchorage elements were cathodic with respect to the strand, substantially aggravating the corrosion of the latter.

7. The corrosion rates determined in the laboratory were consistent with observation of strands failures in the field after only a few years of service, underscoring the corrosion severity that is possible under the mechanisms observed.

8. Rigorous implementation of bleed water avoidance measures is essential in new construction, as well as avoiding design that may promote galvanic corrosion of the strands.

Acknowledgement

The opinions, findings and conclusions expressed here are those of the authors and not necessarily those of the Florida Department of Transportation, the University of South Florida, or the United States Department of Transportation-Federal Highway Administration.

References

Bentur, A., Diamond, S., Berke, N.S., Steel Corrosion in Concrete: Fundamental and Civil Engineering Practice, New York: E & FN Spon, 1997

Corven, J., “Mid Bay Bridge Post-Tensioning Evaluation”, Final Report , Florida Department of Transportation, Tallahassee, October 2001.

Ghorbanpoor, A., Madathanapalli, S. C., "Performance of Grouts for Post-Tensioned Bridge Structures", Report No. FHWA-RD-92-095, National Technical Information Service, Springfield, VA, 1993.

Jones, D.A., Principles and Prevention of Corrosion, 2nd. Ed, Prentice Hall, Upper Saddle River, NJ, 1996.

Kranc, S.C., Sagüés, A.A. "Detailed Modeling of Corrosion Macrocells on Steel Reinforcing in Concrete", Corrosion Science, Vol. 43, p. 1355, 2001.

Li, L., Sagüés, A.A. "Chloride Corrosion Threshold of Reinforcing Steel in Alkaline Solutions - Open-circuit Immersion Tests", Corrosion, Vol. 57, p.19-28, 2001.

Moreno, E.I., Sagüés, A.A., "Carbonation-Induced Corrosion of Blended-Cement Concrete Mix Designs for Highway Structures", Paper No. 636, 10 pp., Corrosion/98, NACE International, Houston, 1998.

Pedeferri, P., "Cathodic Protection and Cathodic Prevention", Construction and Building Materials, Vol. 10, p.391-402, 1996

Powers, R. G., "Corrosion Evaluation of Post-Tensioned Tendons on the Niles Channel Bridge", Florida Department of Transportation, Gainesville, FL, June 1999.

Stauder, A. , Hartt, W.H., "Cathodic Protection of Pre-Tensioned Concrete: Part I - Brittle Failure Propensity of Corrosion Damaged Prestressing Tendon Wire", Paper No. 635, Corrosion/98, Nace International, Houston, 1998.

Szklarska-Smialowska, Z., Pitting Corrosion of Metals, NACE Intnl., Houston, 1986
Tabatabai, H., Ciolko, A. T., and Dickson, T. J., "Implications from Full-Scale Fatigue Tests of Cable Stays Composed of Seven-Wire Prestressing Strands", Proceedings of the Fourth Intnl. Bridge Engineering Conference, Vol. 1, August 28-30, 1995, pp. 266-277.

Vermaas, G., Betti, R., Barton, S.C., Duby, P., West, A.C., "Corrosion and Embrittlement of High-Strength Bridge Wires", p. 85 in Long Term Durability of Structural Materials, Monteiro, P., Chong, K, Larsen-Basse, J. and Komvolopoulos, Eds., Elsevier, Amsterdam, 2001.

Table 1. Summary of Corrosion Test Results

Recharge Event	No. 1		No. 2				No. 3			Dry Values	No. 4			No. 5		
Water added on day	6		7				56				113			117		
DI Water added (mL)	200		100				150				200			200 with 1000 ppm Cl^-		
Initial depth of water	1.25		0.6				1				1.25			1.25		
Water reabsorbed by day	7		9				83 or earlier				115			118		
Conditions on day	6	7	8	9	26	56	56.1	57	83	106	114	115	117	119	131	166
Anchorage Potential (mV vs CSE)	-518	-463	-600	-431	-197	2	-577	-557	-412	-248	-648			-603		
Strand Potential (mV vs CSE)	-537	-466	-549	-485	-221	0	-463	-629	-423	-225	-625			-558		
Macrocell Current[1] (μA)	-140	-10	470	-130	-20	nil	1120	-810	-270	4	304	-331	-105	136	-525	-145
Anchorage Nominal Corrosion Current[1] (From Rp test) (μA)										20	1656			2214		
Strand Nominal Corrosion Current[1] (From Rp test) (μA)										17	749			875		
System Nominal Corrosion Current[1] (From Rp test) (μA)										27	2142			2176		
Strand Pitting Rate[2] (mm/yr)	0.53															

Notes: 1. Negative current value indicates strand is anode.
2. Pitting rate of strands based on average maximum pit depth (Figure 13)

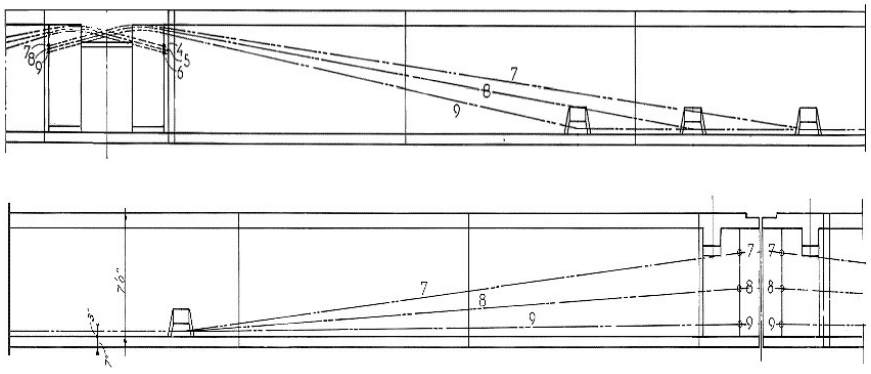

Figure 1 – Typical tendon configuration in the superstructure of the affected bridges.

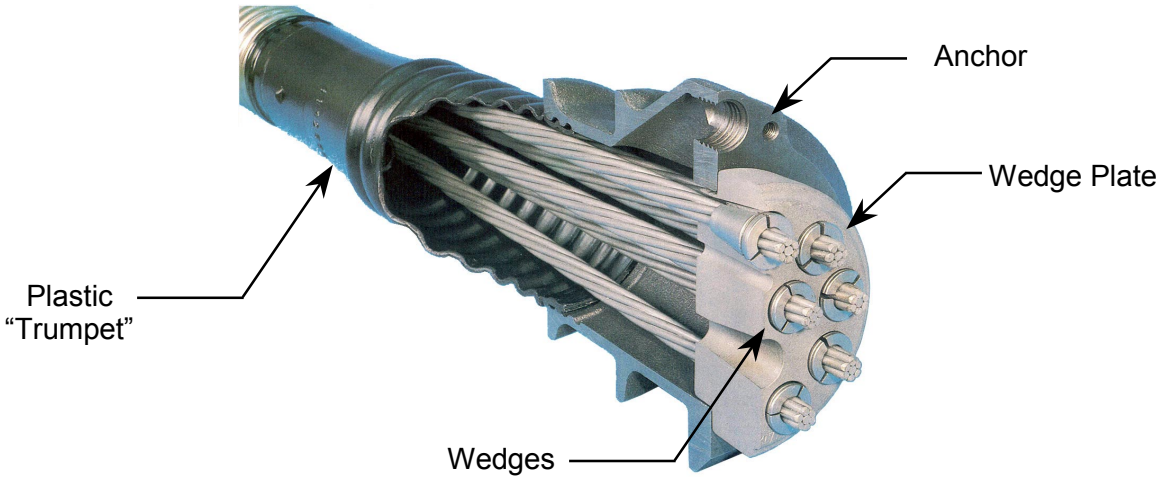

Figure 2 – Details of the anchorage system used in the Niles Channel and Mid Bay Bridges.

Figure 3 – Failed tendon-Niles Channel Bridge (June, 1999).

Figure 4 – Anchor at failed tendon showing chalky grout, partial grout filling and heavy corrosion.

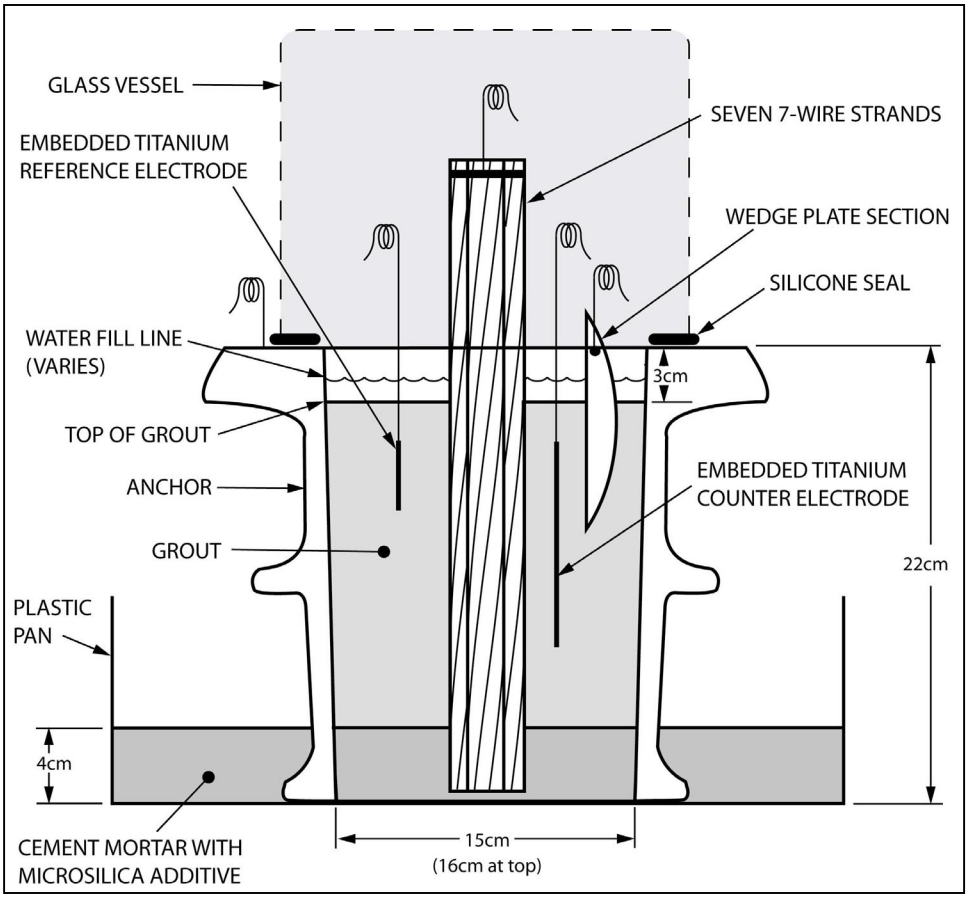

Figure 5 – Schematic of the experimental anchorage mock-up.

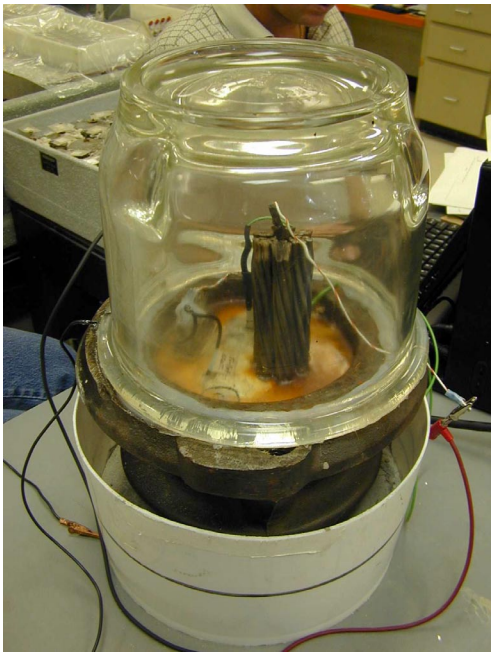

Figure 6 – Photograph of the experimental anchorage mock-up.

Figure 7 – Photograph of the test apparatus for measuring grout bleed-water and grout volume change.

Figure 8 – Photograph depicting increasing chalkiness toward the top of the aluminum admixed grout (vibrated).

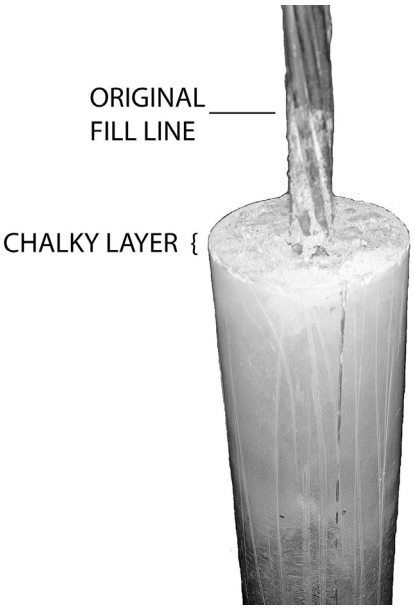

Figure 9 – Close-up photograph depicting large grout volume loss and heavy chalk development in the aluminum admixed grout (vibrated).

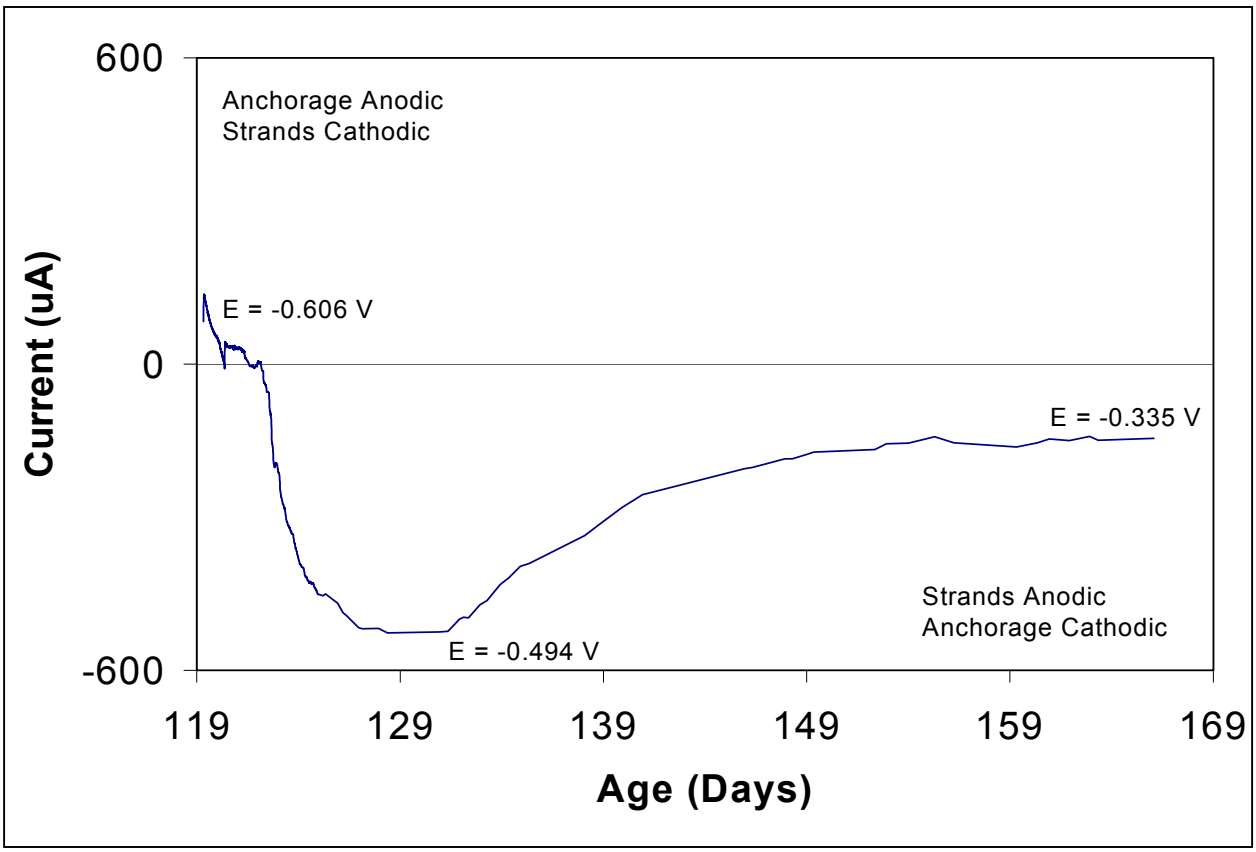

Figure 10 – Macro-cell current and half-cell potentials for the fifth water re-charge event.

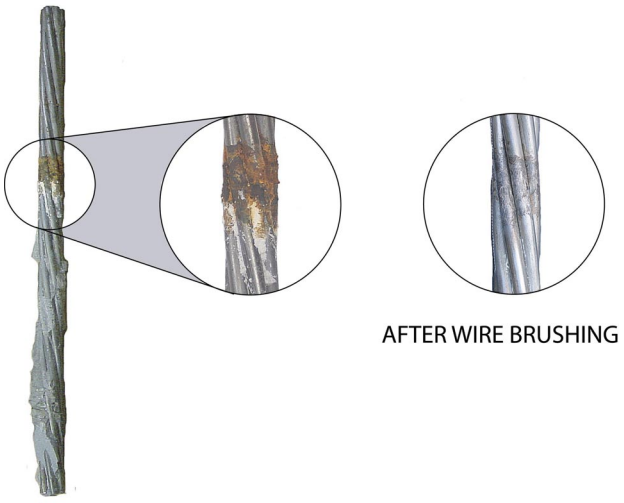

Figure 11 – Typical appearance of the strand upon removal from the mock-up.

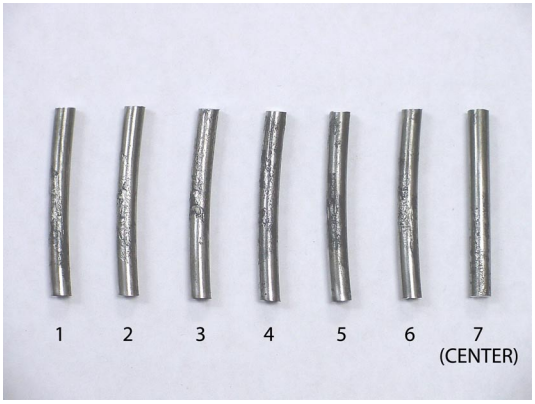

Figure 12 – Typical appearance of the corrosion pits on the strands near the top of the grout.

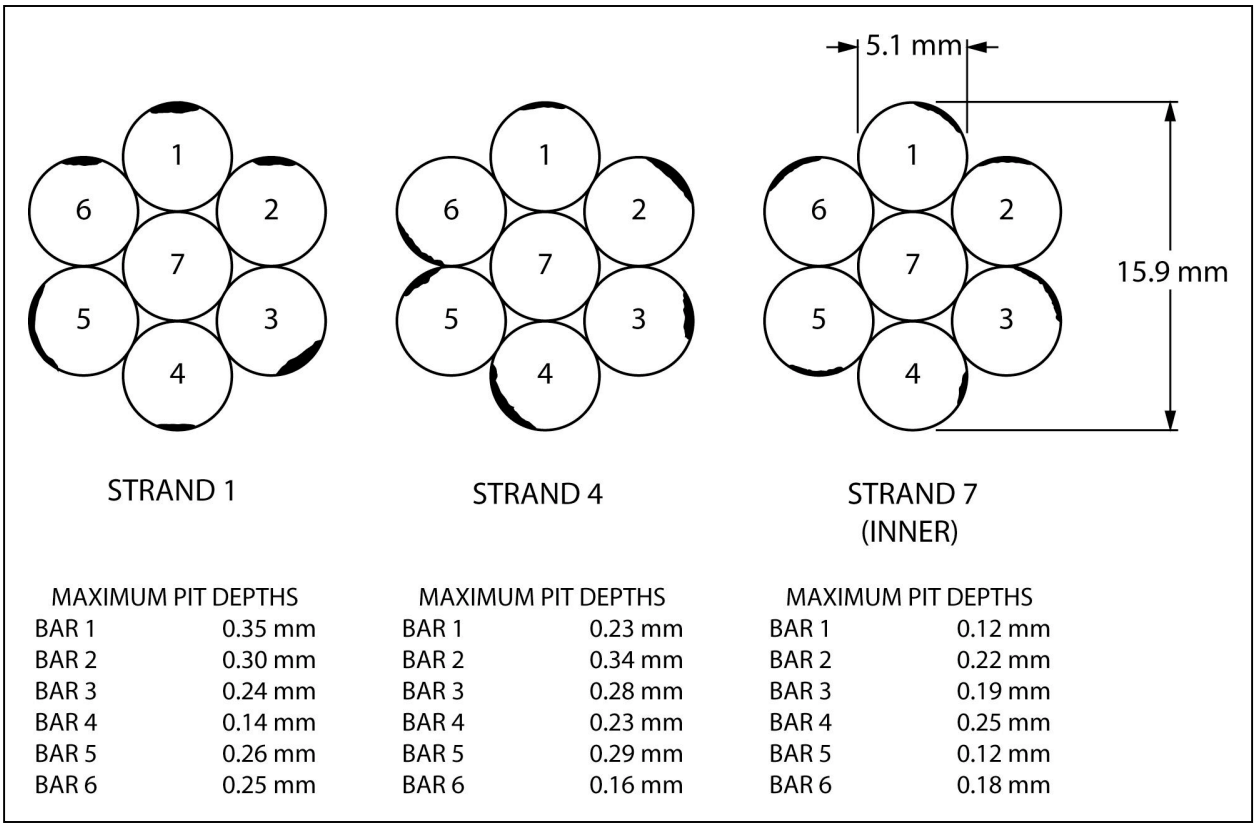

Figure 13 – Schematic representation of the maximum observed corrosion pitting for each of the wires of the three selected strands.